The Reflection from an Open-Ended Rectangular Waveguide Terminated by a Layered Dielectric Medium

VIRON TEODORIDIS, THOMAS SPHICOPOULOS, AND FRED E. GARDIOL, SENIOR MEMBER, IEEE

Abstract—**The measurement of reflection from an open-ended waveguide is a simple and nondestructive technique for determining the dielectric properties of materials. A flange-mounted waveguide is considered, the flange being pressed on an unknown material which may be of finite or infinite thickness. The relationship linking the reflection coefficient to the dielectric properties is obtained from a theoretical analysis of the electromagnetic field in the vicinity of the aperture. The theory includes the effects of both cross polarization and higher order modes. An integral equation is obtained, the kernel of which is the dyadic Green function in each medium. The method of characteristic modes is used for the numerical computation. The theoretical results are in good agreement with experimental measurements. Furthermore, a simple and handy technique for data inversion is provided.**

I. Introduction

TODAY, open-ended waveguides are used in a number of new applications of microwaves and millimeter waves to the fields of material measurements and biomedical engineering. Among these are the nondestructive measurement of material properties and medical techniques such as thermography and hyperthermia. Indeed, the dielectric properties of an unknown material or biological tissue can be determined in a noninvasive way from a measured reflection coefficient, provided a theoretical relation to the dielectric properties of the material is available.

The radiation from a waveguide covered by a dielectric slab received considerable attention several years ago in order to understand the behavior of antennas on space vehicles during the reentry into the Earth's atmosphere. The open-ended rectangular waveguide radiating through a dielectric slab [1]–[3] or directly into the half-space [4], [5] was first treated approximately by variational methods. These publications only considered the contribution of the dominant mode in the aperture field.

Later on, the analysis of the rectangular waveguide radiating into an infinite dielectric material was made including higher order modes [6]–[12], but cross polarization was not always taken into account [6], [11]. A number of mathematical formulations associated with different physical models have been used to describe the problem, and various numerical techniques have been applied. Indeed, beside variational methods [9]–[11], an integral formulation was developed [6]–[8] as well as a matrix correlation method [12]. Furthermore, a physical model considering the half-space as a second waveguide of a very large cross section was proposed [13]. We do not quote here a number of papers modeling the rectangular waveguide as a parallel plate waveguide. Such an approach neglects, among other effects, the cross-polarized electric field.

The rectangular waveguide radiating into a layered medium aroused less attention. A rigorous development including higher order modes and cross polarization was made for the dielectric coated waveguide antenna by means of a variational principle [9]. More recently, a method using the model of the transition to an oversized waveguide was suggested for the study of applicators for multilayered configuration of tissues [14].

This paper presents an integral formulation applicable either to a stratified or an infinite dielectric medium. The actual field distribution is considered, including higher order modes as well as cross polarization. Furthermore, the contribution of surface waves appears explicitly and the formulation is suitable for near field calculations.

Boundary conditions specifying the continuity of the tangential field components yield an integral equation, the kernel of which is the dyadic Green function inside and outside the waveguide. This equation is solved by the method of characteristic modes [17], which yields an eigenvalue equation independent of the excitation.

The solution of the field equation yields the reflection coefficient for a known dielectric medium, while the solution of the inverse problem is needed in practice. Hence, we propose here a simple method for the computation of the complex permittivity corresponding to a measured reflection coefficient.

II. Geometry and Assumptions

The geometry of the problem involves an internal and an external region, separated by an infinite conducting plane. The internal region is the inside of the rectangular wave-

Manuscript received July 20, 1984; revised December 5, 1984. This work was supported in part by the Swiss National Research Foundation under Grant 2.459-0.82.

V. Teodoridis is with the Centre Suisse d'Electronique et de Microtechnique SA., CH-2000 Neuchâtel 7, Switzerland.

T. Sphicopoulos and F. E. Gardiol are with the Laboratoire d'Electromagnetisme et d'Acoustique Ecole Polytechnique Fédérale de Lausanne, Lausanne 1007, Switzerland.

0018-9480/85/0500-0359$01.00 ©1985 IEEE

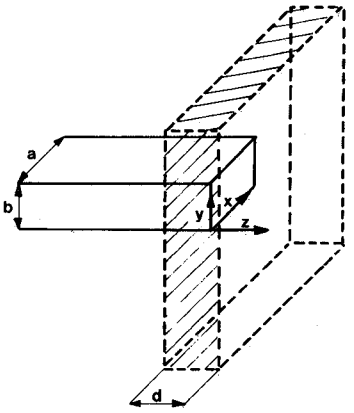

Fig. 1. Geometry of the problem.

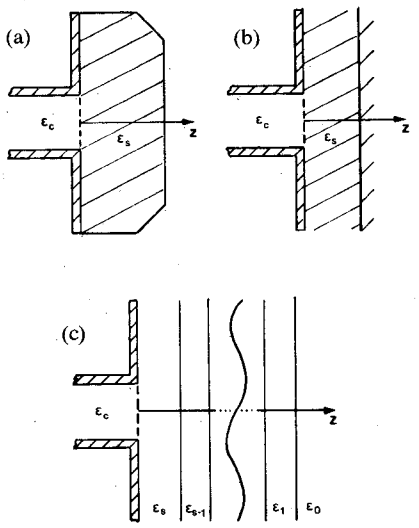

Fig. 2. The three basic configurations.

guide, while the external one is the half-space filled by an isotropic and nonmagnetic dielectric medium (Fig. 1). A metallic flange terminating the waveguide is represented by the infinite conducting plane. The aperture itself is modeled as an equivalent magnetic current flowing on the uninterrupted conducting plane. This current radiates into both regions, and couples the dominant mode in the waveguide to higher order modes. The transverse electric field may be either parallel or cross polarized with respect to the dominant mode. Furthermore, we assume that the incident wave propagates through the dominant mode of the waveguide, filled with a lossless dielectric of permittivity ϵ_c.

The external dielectric medium may be lossy or not, and fills the half-space $z > 0$. We have considered three different configurations (Fig. 2):

a) infinite dielectric medium of permittivity ϵ_s filling the whole half-space,
b) a dielectric medium of finite thickness d, but with infinite transverse dimensions terminated by a metallic plane parallel to the flange,
c) a dielectric medium of finite thickness and unterminated, yielding a stratified structure.

III. Integral Equation and Method of Resolution

The aperture, as seen from the outside ($z > 0$), is replaced by a perfectly conducting metallic wall on which flows an equivalent magnetic surface current $\vec{M}_e$. Similarly from the inside, we consider a short-circuit plate termination on which flows a surface current $\vec{M}_{\text{int}}$. Applying the continuity condition of the tangential magnetic field on the aperture, one obtains [16]

$$\vec{H}_1(\vec{r}) = -\frac{1}{2}\int_{S'}\left[\bar{\bar{G}}(\vec{r},\vec{r}') + \bar{\bar{B}}(\vec{r},\vec{r}')\right]\cdot\vec{M}(\vec{r}')\,dS'. \quad (1)$$

$\bar{\bar{G}}$ represents the external dyadic Green function in the dielectric medium and $\bar{\bar{B}}$ the internal dyadic Green function in the waveguide. S' is the aperture area, $\vec{H}_1$ the transverse component of the incident magnetic field. The equivalent magnetic current $\vec{M}$ is proportional to the actual tangential electric field in the aperture $\vec{E}_a$. Thus, one may write

$$\vec{H}_1 = U_0 Y_1 \vec{W}_1 \quad (2a)$$

$$\vec{M} = -\vec{M}_e = \vec{M}_{\text{int}} = \vec{e}_z \times \vec{E}_a = U_0\left[\vec{W}_1 + \sum_{n=1}^{\infty}\Gamma_n\vec{W}_n\right] \quad (2b)$$

where the $\vec{W}_n$ are the orthogonal transverse dependence functions of the magnetic field, Γ_1 is the reflection coefficient of the dominant mode, Γ_n the relative amplitudes of the higher order evanescent modes, U_0 the amplitude of the incident wave, and Y_1 its wave admittance.

Taking the scalar product of the incident field by the magnetic current and applying orthogonality conditions for the $\vec{W}_n$, one obtains for the reflection coefficient Γ_1

$$\Gamma_1 = \left(U_0^2 Y_1\right)^{-1} < \vec{H}_1, \vec{M} > -1. \quad (3)$$

An expression equivalent to (3) may be obtained for the equivalent admittance of the aperture. Indeed, (1) may be written as [16]

$$\vec{H}_1 = -\left[1/(1-\Gamma_1)\right]\int_{S'}\left[\bar{\bar{G}}(\vec{r},\vec{r}') + \bar{\bar{B}}_0(\vec{r},\vec{r}')\right]\cdot\vec{M}'\,dS' \quad (4)$$

where $\bar{\bar{B}}_0$ is obtained by omitting the dominant-mode term in $\bar{\bar{B}}$.

Taking the scalar product of (4) by the magnetic current, one obtains, using (3)

$$\frac{Y}{Y_1} = \frac{1-\Gamma_1}{1+\Gamma_1} = -U_0^2 Y_1 \frac{\int_S\int_{S'}\vec{M}\cdot\left(\bar{\bar{G}} + \bar{\bar{B}}_0\right)\cdot\vec{M}'\,dS\,dS'}{\left[\int_S \vec{M}\cdot\vec{H}_1\,dS\right]^2}. \quad (5)$$

Equations (1)–(5) are the mathematical expressions which describe the physical problem, as defined in Section II. The method of characteristic modes is used for their resolution.

The characteristic mode currents of a structure form a set of equations particular to the geometry of the structure and independent of the excitation. They are the solutions of an eigenvalue equation, which may be expressed in matrix form after projection onto a set of arbitrary base functions. Their scalar product with the excitation yields the actual current on the structure.

Let y_{op} stand for either the integral operator in (1) or (4). It may be written as

$$y_{op}(\vec{M}) = g_{op}(\vec{M}) + jb_{op}(\vec{M}) \tag{6}$$

where g_{op} and b_{op} are real symmetric operators and g_{op} must be a positive semi-definite operator, since the power radiated by $\vec{M}$ on S is positive semi-definite [18]. The current $\vec{M}$ may be expressed as a linear combination of the characteristic currents $\vec{M}_k$, and an eigenvalue equation is obtained [17]

$$b_{op}(\vec{M}_k) = \lambda_k g_{op}(\vec{M}_k) \tag{7}$$

where the power radiated by each characteristic current is considered to be unitary.

The arbitrary set of base functions used to expand the characteristic currents is chosen to be the set of transverse modal functions in the waveguide. The projection of the characteristic currents on the base functions yields

$$\vec{M}_k = \sum_n u_{kn}\vec{W}_n \tag{8}$$

where u_{kn} are unknown constants.

The scalar product of (7) by $\vec{M}_m$, and replacement of the characteristic currents by their series expansion (8), yields a matrix equation

$$[b][u_k] = \lambda_k[g][u_k] \tag{9}$$

in which the matrix elements are

$$b_{mn} = \langle \vec{W}_m, b_{op}(\vec{W}_n)\rangle \quad g_{mn} = \langle \vec{W}_m, g_{op}(\vec{W}_n)\rangle. \tag{10}$$

The resolution of this equation [18], yields the eigenvalues λ_k and eigenfunctions $\vec{u}_k$. The actual current $\vec{M}$, however, is a function of the excitation. We define now the coefficients I_k by

$$I_k = \langle \vec{M}_k, \vec{H}_1\rangle \tag{11}$$

and the actual magnetic current $\vec{M}$ is found to be [17]

$$\vec{M} = \sum_k \frac{I_k}{(1+j\lambda_k)}\vec{M}_k. \tag{12}$$

Once eigenvalues and eigenfunctions are found from (9), the reflection coefficient and the aperture admittance may be computed from (3) or (5) using (12), (8), and (2a), yielding the relations

$$\Gamma_1 = Y_1\sum_k \frac{u_{k1}^2}{(1+j\lambda_k)} - 1 \quad \frac{Y}{Y_1} = \left(Y_1\sum_k \frac{u_{k1}^{*2}}{(1+j\lambda_k^*)}\right)^{-1} \tag{13}$$

where $\vec{u}_{k1}$ and λ_k stand for the eigenfunctions and eigenvalues found from the integral operator defined in (1), while $\vec{u}_{k1}^*$ and λ_k^* are associated with the integral operator defined in (4).

IV. Dyadic Green Functions

When both components of the electric field on the aperture are considered and when, furthermore, the near field distribution is to be evaluated, a dyadic Green function must be used in the integral equation instead of the scalar one.

The external dyadic Green function $\bar{\bar{G}}$ takes different forms, according to the geometry of the dielectric medium, while $\bar{\bar{B}}$ is the dyadic Green function in the rectangular waveguide. When only the transverse part of $\bar{\bar{B}}$ is needed, a simple expression may be found [16]

$$\bar{\bar{B}}_t(\vec{r},\vec{r}') = -\sum_{n=1}^{\infty} Y_n\vec{W}_n(\vec{r}_t)\vec{W}_n(\vec{r}_t')\exp(-\gamma_n|z-z'|). \tag{14}$$

In the homogeneous case, $\bar{\bar{G}}$ has the well-known form

$$\bar{\bar{G}} = j\omega\epsilon_0\left(\bar{\bar{I}} + \frac{\nabla\nabla}{k_s^2}\right)\psi \tag{15}$$

where $\psi = \exp(-jk_sR)/2\pi R$, $k_s^2 = \epsilon_s\epsilon_0\mu_0\omega^2 = \epsilon_s k_0^2$, and $R = |\vec{r}-\vec{r}'|$.

In the metal-bounded case, $\bar{\bar{G}}$ is still given by (15), but ψ is given by the image method

$$\psi = \exp(-jk_sR)/2\pi R + 2\sum_{n=1}^{\infty}\exp(-jk_sR_n)/2\pi R_n \tag{16}$$

where

$$R_n^2 = R^2 + (2nd)^2.$$

In the case of the stratified medium, finally, it can be shown that $\bar{\bar{G}}$ may be separated into TM(E) and TE(H) parts yielding for its transverse part [15], [21]

$$\bar{\bar{G}}_t(R,\phi) = j\omega\epsilon_0\int_0^{\infty}\bar{\bar{g}}(\lambda,R,\phi)\lambda\,d\lambda \tag{17a}$$

where

$$\begin{aligned}
\bar{\bar{g}} &= C^E\bar{\bar{g}}^E + C^H\bar{\bar{g}}^H\\
g_{xx}^E &= -g_{yy}^H = J_0(\lambda R) + J_2(\lambda R)\cos 2\phi\\
g_{xy}^E &= g_{yx}^E = g_{xy}^H = g_{yx}^H = J_2(\lambda R)\sin 2\phi\\
g_{yy}^E &= -g_{xx}^H = J_0(\lambda R) - J_2(\lambda R)\cos 2\phi.
\end{aligned} \tag{17b}$$

In the case of N layers, (Fig. 2(c)) numbered from 0 to s ($s = N-1$), one may find that $C^{E,H}$ in the source layer is given by

$$C_s^{E,H} = \frac{\alpha_s^{E,H}\exp[-U_s(z-h_s)] + \beta_s^{E,H}\exp[U_s(z-h_s)]}{\alpha_s^{E,H}\exp(U_sh_s) - \beta_s^{E,H}\exp(-U_sh_s)} \tag{18a}$$

where the coefficients have to be determined recursively

$$\begin{pmatrix}\alpha_n\\ \beta_n\end{pmatrix}^{E,H} = \begin{pmatrix}(1+\psi_n^{E,H})\exp(U_{n-1}h_{n-1}) & (1-\psi_n^{E,H})\exp(-U_{n-1}h_{n-1})\\ (1-\psi_n^{E,H})\exp(U_{n-1}h_{n-1}) & (1+\psi_n^{E,H})\exp(-U_{n-1}h_{n-1})\end{pmatrix}\begin{pmatrix}\alpha_{n-1}\\ \beta_{n-1}\end{pmatrix}^{E,H} \tag{18b}$$

$n \in (1, s)$, h_n being the nth layers thickness $z' = 0$ and

$$\psi_n^H = \frac{U_n}{U_{n-1}} \quad \psi_n^E = \frac{\epsilon_n}{\epsilon_{n-1}} \frac{U_{n-1}}{U_n}$$

$$\begin{pmatrix} \alpha_1 \\ \beta_1 \end{pmatrix}^{E,H} = \begin{pmatrix} 1+\psi_1 \\ 1-\psi_1 \end{pmatrix}^{E,H} \qquad U_n^2 = \lambda^2 - \epsilon_n k_0^2. \quad (18c)$$

On the other hand, for $z = 0$, $C_s^{E,H}$ itself is to be found recursively in a simpler form

$$C_n^{E,H} = \frac{C_{n-1}^{E,H} + \psi_n^{E,H} \tanh U_n h_n}{\psi_n^{E,H} + C_{n-1}^{E,H} \tanh U_n h_n} \qquad (19)$$

starting with $C_o = 1$.

In the case of two layers, the corresponding coefficients of the TE and TM parts for $z = 0$ are given by

$$C^E = \frac{\epsilon_s}{4\pi} \frac{\epsilon_s U_0 \tanh U_s d + U_s}{U_s (U_s \tanh U_s d + \epsilon_s U_0)}$$

$$C^H = \frac{\epsilon_s U_s}{4\pi k_s^2} \frac{U_s \tanh U_s d + U_0}{U_0 \tanh U_s d + U_s} \qquad (20a)$$

where

$$U_s^2 = \lambda^2 - k_s^2 \quad U_0^2 = \lambda^2 - k_0^2 \quad d = h_1. \qquad (20b)$$

V. Admittance Matrix

The computation of the matrix elements in (9) presents several difficulties. In the homogeneous and in the metal-bounded cases, the external dyadic Green function has a singularity at the origin with a $1/R^3$ behavior, due to the taking of a double derivative (15). Both derivatives may be avoided by applying an integral identity, after projection of the integral equation on the base functions. This allows one to differentiate the base functions instead of the ψ in (15) [16].

The matrix elements are the result of two double integrations over the aperture. The external term is integrated twice analytically after a change of coordinates [4]. The remaining two integrations must be performed numerically. The $1/R$ singularity in the imaginary part of the operator is finally suppressed after transformation to polar coordinates. For the internal term, on the other hand, numerical integrations are not needed and the nondiagonal terms vanish.

The admittance matrix $[y] = [g] + j[b]$ is written as

$$[y] = \begin{pmatrix} [y^{xx}] & [y^{xy}] \\ [y^{yx}] & [y^{yy}] \end{pmatrix} \qquad (21)$$

the matrix elements being

$$y_{ij}^{\mu\nu} = -\frac{1}{2j\omega\mu_0} \left[\int_0^{\alpha} \int_0^{a/\cos\phi} F_{ij}^{\mu\nu}(p, q) + \int_{\alpha}^{\pi/2} \int_0^{b/\sin\phi} F_{ij}^{\mu\nu}(p, q) \right] \psi R \, dR \, d\phi + Y^{\mu\nu} \delta_{ij} \qquad (22)$$

where

$$p = x - x' = R\cos\phi \quad q = y - y' = R\sin\phi$$

$$\alpha = \arctan b/a \quad \mu, \nu \equiv x, y$$

$$F_{ij}^{xx} = \left(k_s^2 f_3^{ij} - \frac{m_i m_j \pi^2}{a^2} f_1^{ij} \right) f_2^{ij} \quad F_{ij}^{xy} = -\frac{m_i l_j \pi^2}{ab} f_1^{ij} f_2^{ij}$$

$$F_{ij}^{yx} = -\frac{l_i m_j \pi^2}{ab} f_1^{ij} f_2^{ij} \quad F_{ij}^{yy} = \left(k_s^2 f_4^{ij} - \frac{l_i l_j \pi^2}{b^2} f_2^{ij} \right) f_1^{ij} \qquad (23a)$$

and

$$f_{\frac{1}{3}}^{ij} = \frac{a}{\pi} \left[S_j(p)(1/m_d \mp 1/m_s) - S_i(p)(1/m_d \pm 1/m_s) \right]$$

$$f_{\frac{2}{4}}^{ij} = \frac{b}{\pi} \left[S_j(q)(1/l_d \mp 1/l_s) - S_i(q)(1/l_d \pm 1/l_s) \right] \qquad (23b)$$

if $m_i = m_j$ and/or $l_i = l_j$ one obtains

$$f_{\frac{1}{3}}^{i} = \mp \frac{a}{\pi m_i} S_i(p) + (a - p) C_i(p)$$

$$f_{\frac{2}{4}}^{i} = \mp \frac{b}{\pi l_i} S_i(q) + (b - q) C_i(q)$$

if

$$l_i = l_j = 0 \quad f_2 = 2(b - q) \quad f_4 = 0. \qquad (23c)$$

The following definitions have been used:

$$\begin{matrix} S_i \\ C_i \end{matrix}(p) = \begin{cases} \sin\left(\frac{\pi}{a} m_i p\right) \\ \cos\left(\frac{\pi}{a} m_i p\right) \end{cases} \quad \begin{matrix} S_i \\ C_i \end{matrix}(q) = \begin{cases} \sin\left(\frac{\pi}{b} l_i q\right) \\ \cos\left(\frac{\pi}{b} l_i q\right) \end{cases} \qquad (23d)$$

$$m_s = m_i + m_j \quad l_s = l_i + l_j, \qquad m: \text{odd}$$

$$m_d = m_i - m_j \quad l_d = l_i - l_j, \qquad l: \text{even}.$$

Finally, for the internal part, it can be found that

$$Y^{xx} = -\frac{1}{2j\omega\mu_0} \frac{ab\pi}{8} \frac{\epsilon_{om}\epsilon_{ol}}{\gamma_k} \left[\left(\frac{m_i \pi}{a} \right)^2 - k_c^2 \right]$$

$$Y^{xy} = Y^{yx} = -\frac{1}{2j\omega\mu_0} \frac{\pi^3 \epsilon_{om}\epsilon_{ol}}{8\gamma_k} \cdot m_i l_i$$

$$Y^{yy} = -\frac{1}{2j\omega\mu_0} \frac{ab\pi}{8} \frac{\epsilon_{om}\epsilon_{ol}}{\gamma_k} \left[\left(\frac{l_i \pi}{b} \right)^2 - k_c^2 \right] \qquad (24a)$$

with

$$\gamma_k = \sqrt{\left(\frac{m_i \pi}{a} \right)^2 + \left(\frac{l_i \pi}{b} \right)^2 - k_c^2}$$

$$k_c = \sqrt{\epsilon_c} k_0 \qquad (24b)$$

and $\epsilon_{om}, \epsilon_{ol}$ stand for Newmann factors

$$\epsilon_{om,l} = \begin{cases} 1, & \text{if } m, l = 0 \\ 2, & \text{if } m, l \neq 0. \end{cases}$$

In the stratified case, the dyadic Green function operator does not involve any derivatives, and the integral identity mentioned in the homogeneous case cannot be used. The $1/R^3$ singularity at the origin cannot be avoided. The change of variables is made as in the homogeneous case and the internal part does not change. The general term of

the admittance matrix is also given by (22), but in this case we have

$$F_{ij}^{xx} = g_{xx} f_3^{ij} f_2^{ij} \qquad F_{ij}^{xy} = g_{xy} h_3^{ij} h_2^{ij}$$
$$F_{ij}^{yx} = g_{yx} h_1^{ij} h_4^{ij} \qquad F_{ij}^{yy} = g_{yy} f_1^{ij} f_4^{ij} \tag{25}$$

where

$$h_{\substack{1\\3}}^{ij} = \pm \frac{a}{\pi}\left[C_j(p) - C_i(p)\right]\left[1/m_d \mp 1/m_s\right]$$
$$h_{\substack{2\\4}}^{ij} = \pm \frac{b}{\pi}\left[C_j(q) - C_i(q)\right]\left[1/l_d \mp 1/l_s\right] \tag{26a}$$

when $m_i = m_j$ and/or $l_i = l_j$

$$h_{\substack{1\\3}}^{ij} = \pm (p-a) S_i(p) \quad h_{\substack{2\\4}}^{ij} = \pm (q-b) S_i(q). \tag{26b}$$

Besides the $1/R^3$ singular term at the origin, the dyadic Green function has poles on the real axis of the complex spatial frequency plane when the dielectric is lossless. Therefore, special techniques are necessary to evaluate the infinite integral (17) on this axis. Hence, in the stratified case, the numerical computation of the matrix elements involves this infinite integral in addition to the surface integrations.

VI. Numerical Computations

In order to solve the eigenvalue equation obtained with the characteristic modes method, the surface integrations in the admittance matrix have to be evaluated first. But in the case of a stratified geometry, each contribution to the surface integral is itself the result of an integration over the entire plane of spatial frequencies. The Green function may be expressed in terms of four different spectral integrals, the integrands of which depend only on λR. Expressing $J_2(\lambda R)$ in (17), in terms of J_0 and J_1, one obtains

$$I_0^{E,H} = \int_0^\infty C^{E,H} J_0(\lambda R) \lambda R \, d\lambda$$
$$I_1^{E,H} = \int_0^\infty C^{E,H} J_1(\lambda R) \, d\lambda. \tag{27}$$

In order to avoid prohibitive computation time, the surface integrals are evaluated using interpolated values after a number of integrations on the spatial frequency plane computed for discrete values of R.

The evaluation of these integrals may involve two types of difficulties: there may be poles or a branch point in the integrand; the integrand may oscillate and may diverge for increasing values of the argument.

It is always possible to treat the two problems separately by division of the integration interval.

The following normalizations are made throughout:

$$\lambda = \lambda / k_0 \quad R = k_0 R \quad d = k_0 d. \tag{28}$$

The roots of the complex denominators of C^E and C^H noted D^E and D^H determine the poles of the integrands defined in (27). The roots must be computed precisely in order to ensure an accurate evaluation of the integrals. When the medium is lossless, all the roots lie on the real axis in the interval $\sqrt{\epsilon_{\min}} \leqslant \lambda \leqslant \sqrt{\epsilon_{\max}}$, and a very simple algorithm may be used. In Fig. 3, D^E and D^H versus λ are shown for an example with two layers. The imaginary parts vanish beyond the branch point $\lambda = 1$, where a discontinuity of $D^{E,H}$ is located. On the other hand, $\lambda = \sqrt{\epsilon_s}$ is not a branch point, and thus $D^{E,H}$ and their derivatives are continuous at this point.

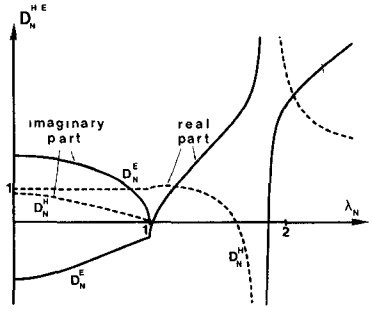

Fig. 3. Normalized values of $D^{H,E}$ versus λ_N. $D_N^{H,E} = D^{H,E}/U_s^{H,E}$, $\lambda_N = \lambda/k_0, \epsilon_s = 4, d = 1$ cm, $f = 10$ GHz.

The number of roots for the two-layer case is predictable and given by

$$Nb^{E,H} = \text{Integer}\left(\frac{k_o d}{\pi} \cdot \sqrt{\epsilon_s - 1} + n_H^E\right) \quad n_H^E = \begin{cases} 1 \\ 0.5 \end{cases}. \tag{29}$$

As a matter of fact, D^E always has at least one root. This means that the first TM surface-wave mode has no cutoff frequency. On the other hand, the D^H has no roots when the following condition is fulfilled: $k_0 d\sqrt{\epsilon_s - 1} < \pi/2$.

The first difficulty in the integration of (27) may be bypassed if the path is deformed on the real axis. The integrals in (27) take the following form, when poles are present:

$$I^{E,H} = PV \int_0^\infty C^{E,H} J_n(\lambda R)[\lambda R]^{(1-n)} d\lambda$$
$$- \pi j \sum_i R_i^{E,H} J_n(\lambda_i R)[\lambda_i R]^{(1-n)}, \qquad n = 0,1 \tag{30}$$

where λ_i is the ith pole of $C^{E,H}$, $R_i^{E,H}$ is the corresponding residue, and PV denotes the principal Cauchy value of the integral. The sum of residues in (30) represents the contribution of TE and TM surface-wave modes and are given by

$$R_i^{E,H} = N^{E,H} \left(\frac{\partial D^{E,H}}{\partial \lambda}\right)^{-1}\Bigg|_{\lambda = \lambda_i} \tag{31}$$

where $N^{E,H}$ stands for the numerator of $C^{E,H}$.

In order to determine numerically the principal value of the integrals, the real axis is first divided into a number of intervals. A symmetrical integration interval centered on each pole is chosen to simplify developments. Furthermore, the branch point must always be the limit of an interval.

These integrals are evaluated by folding the intervals around the poles. It can be shown [19] that the new integrands are no longer singular at the pole location. Neglecting possible numerical errors, the folded interval integration is rigorously equivalent to straight integration with symmetrical points around the pole.

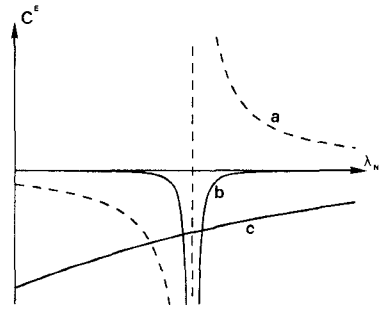

Fig. 4. The effect of the change of variables (33) on the form of C^E. (a) Real part and (b) imaginary part of C^E without any transformation and (c) imaginary part of C^E after the change of variables as defined in (33). $\lambda_N = \lambda/k_0$, $\epsilon_s = 4$, $d = 1$ cm, $\tan\delta = 0.001$, $f = 10$ GHz.

The second difficulty encountered is the treatment of the oscillating integrand, which often diverges over the interval $[A, \infty]$, where $A > \sqrt{\epsilon_{\max}}$. A method specially developed [19] to deal with Sommerfeld integrals is used here.

In the case of a lossy dielectric medium, the poles move slightly away from the real axis, taking a small negative imaginary part. Considering the denominators $D^{E,H}$ in the two-layer case as functions of the complex variables $k_\rho = \lambda + j\nu$ and $\epsilon_s = \epsilon_s'(1 + j\tan\delta)$, and assuming that ν is very small, a Taylor's series expansion around the point $(\lambda_i^0, \epsilon_s')$ gives

$$\lambda_i^{E,H} = \lambda_i^{0E,H} \qquad \nu_i^{E,H} = \epsilon_s' \tan\delta \frac{\partial(D^{E,H})/\partial\epsilon_s}{\partial(D^{E,H})/\partial k_\rho} \tag{32}$$

where the superscript 0 denotes the location of the ith pole in the lossless case.

The accuracy of these approximate formulas is very good for a very large range of $\tan\delta$. When this is not the case, these values may still be used as the initial solution in an optimization process yielding a very fast convergence.

In the lossy case, the pole shift, as small as it may be, changes considerably the numerical procedure for the evaluation of the integral defined in (27). The principal value becomes a regular integral and the residue term vanishes. This fact does not mean that the surface waves vanish too. As a matter of fact they still propagate, but with an exponential attenuation. Furthermore, the integrand is now complex. The real part follows roughly the lossless behavior but vanishes where the singularity was found before. However, the numerical techniques used in the lossless case are still useful. On the other hand, the imaginary part shows a strong peak at $\lambda = \lambda_i$, which cannot be handled by standard numerical integration. To this end we use a change of variables, transforming a strongly peaked behavior into a smooth one [20], which can be integrated numerically without difficulties (Fig. 4). The change of variables is the following:

$$\theta = \operatorname{atan}\left[(\lambda - \lambda_i)/\nu_i\right]. \tag{33}$$

With this technique, the interval of integration around λ_i does not matter anymore for the imaginary part.

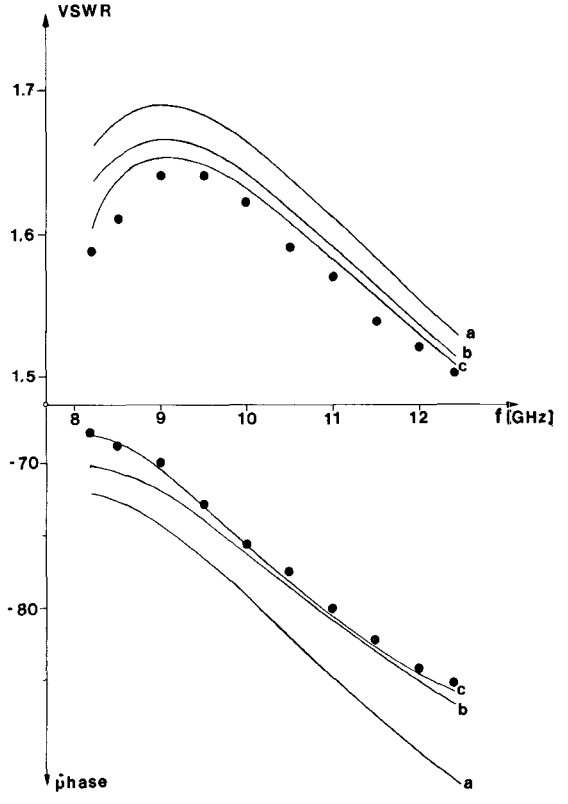

Fig. 5. Comparison of theoretical results for (a) one, (b) three, and (c) ten modes with measured values (●) for radiation in an homogeneous medium (air).

Finally, the singularity of the Green function at the origin ($R = 0$) must be extracted. It can be shown that the singularity in the stratified case is the same as the one for the homogeneous case. Therefore, the singularity is avoided by expressing the dyadic Green function for the stratified geometry as the sum of the homogeneous dyadic Green function with the difference of the two dyadic Green functions. The singularity of the homogeneous term is avoided by treating it in the usual way described in Section V, while the difference term is not singular, provided the homogeneous dyadic Green function is expressed in a form showing its explicit $1/R^3$ behavior.

VII. Numerical Results and Experimental Verifications

The numerical results for the homogeneous case have been checked against experiment by measuring the reflection coefficient versus frequency for the open waveguide radiating into air. The measurements are reported in Fig. 5, and show a very good agreement with theory. In the same figure, comparison is made with theoretical results showing the contribution of higher order modes and of cross polarization. Fig. 6 shows the importance of cross polarization in the stratified medium. Measurements have also been made for dielectric slabs of known properties both with and without a metallic plate. Results and comparison with the theory are shown in Table I.

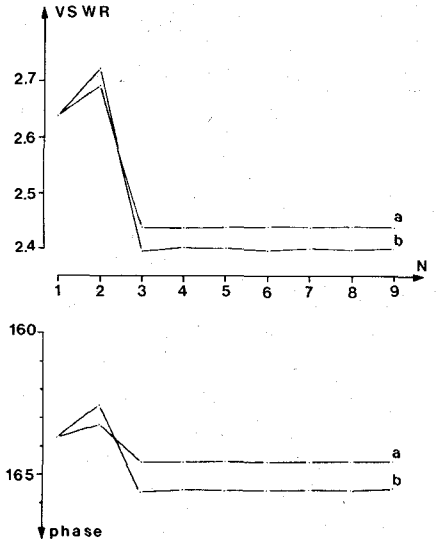

Fig. 6. Convergence of VSWR and phase as a function of the number N of modes considered (a) with and (b) without cross-polarized magnetic current. $\epsilon_s = 4.2$, $\tan\delta = 0.005$, $d = 6.52$ mm, $f = 10$ GHz.

TABLE I

$f = 10$ GHz Dielectric material	Sample measured in waveguide		Metal-backed method		Stratified geometry	
	ϵ_s'	$\tan\delta$	ϵ_s'	$\tan\delta$	ϵ_s'	$\tan\delta$
Stycast 4 $d = 6.52$ mm	4.2	0.005	4.3	0.005	4.2	0.005
Stycast 9 $d = 6.56$ mm	9.6	0.0007	9.8	0.001	9.7	0.0007
Hf 2050 $d = 6.57$ mm	7.5	0.012	7.9	0.008	7.6	0.011
Aracast $d = 9.72$ cm	3.0	0.011	3.1	0.012	3.0	0.010

VIII. Inversion of Computed Data

In order to solve the inverse problem, i.e., deduce the complex permittivity from the measurements of the reflection coefficient, there are two possibilities, if one wishes to avoid the introduction of the complete analysis program into a sluggish optimization loop [11]. For a given frequency, charts similar to that given in [15] and [16] may be computed and plotted. Interpolation between computed points is done graphically. On the other hand, a continuous interpolation can be done from the discrete points on the chart by fitting on them a two-dimensional polynomial [16]. This polynomial approximation is found by a least-square method and may be written as

$$f_p(x, y) = \sum_{i=1}^{3} \sum_{j=1}^{3} C_{ij}^{p} x^i y^i \text{ with } p = \begin{cases} \epsilon_s \\ \tan\delta \end{cases} \qquad (34)$$

where x and y are normalized values of $S \cdot \sin\phi$ and $S \cdot \cos\phi$ ranging between 0 and 1 [16], S standing for the VSWR and ϕ for the phase of the reflection coefficient.

An example of the accuracy provided by the polynomial approximation for an infinite dielectric medium gives 0.2-percent average error for $1.4 \leqslant \epsilon_s \leqslant 10$, and 1.1 percent for $0 \leqslant \tan\delta \leqslant 1$. In the case of a slab, the situation is more complicated, since there are many parameters. The use of the polynomial expansion brings the problem within the range of desktop minicomputers and even of some programmable pocket calculators.

IX. Conclusion

The theory developed here is suitable for both infinite and stratified dielectric media. In practice, a material may be considered as being infinite when the wave diffracted from the aperture is absorbed entirely without further reflection. This condition is verified when the losses and the thickness of the material are large enough. Besides, a slab may or may not be backed by a metallic plate. When losses are small, the metallic back plate is objectionable because it enhances the reflection coefficient, yielding high VSWR. Both cross polarization and higher order modes are taken into account in our analysis and their importance has been shown, particularly in the stratified case.

Special numerical techniques are used for the calculation of the dyadic Green function in a stratified medium, and particular attention is given to the numerical computation for a lossy medium.

Finally, experimental results are in very good agreement with computed values, and an inversion technique, very attractive and suitable for a number of applications, is proposed.

Acknowledgment

The authors wish to thank the Swiss National Research Foundation and Dr. J. R. Mosig for many helpful and constructive discussions.

References

[1] J. Galejs, "Admittance of a waveguide radiating into stratified plasma," *IEEE Trans. Antennas Propagat.*, vol. AP-13, pp. 64–70, Jan. 1965.

[2] W. F. Croswell, R. C. Rudduck, and D. M. Hatcher, "The admittance of a rectangular waveguide radiating into a dielectric slab," *IEEE Trans. Antennas Propagat.*, vol. AP-15, pp. 627–633, Sept. 1967.

[3] W. F. Croswell, W. C. Taylor, C. T. Swift, and C. R. Cockrell, "The input admittance of rectangular waveguide-fed aperture under an inhomogeneous plasma: Theory and experiment," *IEEE Trans. Antennas Propagat.*, vol. AP-16, pp. 475–487, July 1968.

[4] L. Lewin, *Advanced Theory of Waveguides*, London, England: Iliffe, 1951, ch. 6. pp. 121–144.

[5] R. T. Compton, "The admittance of aperture antennas radiating into lossy media," Rep. 1691-5, Ohio State Univ., Antenna Lab. Research Foundation, Mar. 1964.

[6] R. J. Mailloux, "Radiation and near field coupling between two collinear open ended waveguides," *IEEE Trans. Antennas Propagat.*, vol. AP-17, pp. 49–55, Jan. 1969.

[7] R. J. Mailloux, "First order solution for mutual coupling between waveguides which propagate two orthogonal modes," *IEEE Trans. Antennas Propagat.*, vol. AP-17, pp. 740–746, Nov. 1969.

[8] J. R. Mautz and R. F. Harrington, "Transmission from a rectangular waveguide into half-space through a rectangular aperture," *IEEE Trans. Microwave Theory Tech.*, vol. MTT-26, pp. 44–45, Jan. 1978.

[9] D. G. Bodnar and D. T. Paris, "New variational principle in electromagnetics," *IEEE Trans. Antennas Propagat.*, vol. AP-18, pp. 216–223, Mar. 1970.

[10] A. R. Jamieson and T. E. Rozzi, "Rigorous analysis of cross polarization in flange-mounted rectangular waveguide radiators," *Electron. Lett.*, vol. 13, pp. 742–744, Nov. 24, 1977.

[11] M. C. Decreton and F. E. Gardiol, "Simple non-destructive method for the measurement of complex permittivity," *IEEE Trans. Instrum. Meas.*, vol. IM-23, pp. 434–438, Dec. 1974.
[12] R. H. McPhie and A. I. Zaghloul, "Radiation from a rectangular waveguide with infinite flange: Exact solution by correlation matrix," *IEEE Trans. Antennas Propagat.*, vol. AP-28, pp. 497–503, July 1980.
[13] J. Audet, J. C. Bolomey, C. Pichot, D. D. Nguyen, M. Robillard, M. Chive, and Y. Leroy, "Electrical characteristics of waveguide applicators for medical applications," *J. Microwave Power*, vol. 15, pp. 177–186, Sept. 1980.
[14] J. M. Rebollar, "Design of waveguide applicators for medical applications considering multilayered configurations of tissues," in *Proc. Int. URSI Symp.*, 1983, pp. 669–672.
[15] V. Teodoridis, T. Sphicopoulos, and F. E. Gardiol, "The reflection of open ended rectangular waveguides covered by a dielectric slab. Application to non destructive measurement of lossy media," in *Proc. Int. URSI Symp.*, 1983, pp. 573–576.
[16] F. E. Gardiol, T. Sphicopoulos, and V. Teodoridis, "The reflection of open ended circular waveguides—Application to nondestructive measurement of materials," in *Reviews of Infrared and Millimeter Waves*, K. J. Button, Ed., vol. 1. New York: Plenum, 1983, pp. 325–364.
[17] R. F. Harrington and J. R. Mautz, "Theory of characteristic modes for conducting bodies," *IEEE Trans. Antennas Propagat.*, vol. AP-19, pp. 622–628, Sept. 1971.
[18] R. F. Harrington and J. R. Mautz, "Computation of characteristic modes for conducting bodies," *IEEE Trans. Antennas Propagat.*, vol. AP-19, pp. 629–639, Sept. 1971.
[19] J. R. Mosig and F. E. Gardiol, "A dynamical radiation model for microstrip structures," in *Advances in Electronics and Electron Physics*, vol. 59. New York: Academic, 1982, pp. 139–237.
[20] J. R. Mosig and F. E. Gardiol, "Dielectric losses, ohmic losses and surface wave effects in microstrip antennas," in *Proc. Int. URSI Symp.*, 1983, pp. 425–428.
[21] T. Sphicopoulos, V. Teodoridis, and F. E. Gardiol, "A tractable form of the dyadic Green function for application to multilayered isotropic media," *Electron. Lett.*, vol. 19, no. 24, pp. 1055–1057, Nov. 24, 1983, and vol. 20, no. 9, p. 387.

✤

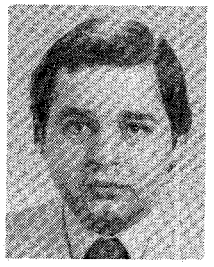

Viron Teodoridis was born in Istanbul, Turkey, on May 20, 1952. He received the Electrical Engineer degree in 1976, and the Doctor in Technical Sciences degree in 1984, both from the Ecole Polytechnique Fédérale de Lausanne (EPFL), Switzerland.

Since 1976, he has been a Research Associate at the Laboratory of Electromagnetism and Acoustics at the EPFL. His main research interests are propagation and scattering of electromagnetic waves and nondestructive material measurement methods.

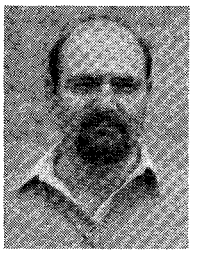

Thomas Sphicopoulos was born in Athens, Greece, in 1953. He received the physics degree in 1976 from the University of Athens, Athens, Greece. In 1977, he received the "Diplôme d'études approfondies" (DEA) in electronics (option microwaves), and in 1980 the "Doctorat de troisième cycle" from the University Pierre et Marie Curie (Paris VI).

He worked on microwave antennas design for the Thomson CSF corporation in France from 1977–1980. He is now with the Laboratoire d'Électromagnétisme et d'Acoustique of the Ecole Polytechnique Fédérale de Lausanne, Switzerland.

✤

Fred E. Gardiol (S'68–M'69–SM'74) was born in Corsier-sur-Vevey, Switzerland, on December 2, 1935. He received the physicist engineer degree of the Ecole Polytechnique de l'Université de Lausanne in 1960, the Master of Science degree at the Massachusetts Institute of Technology, Cambridge, in 1965, and the Doctor degree in applied science from the Catholic University of Louvain, Belgium in 1969.

He worked as an Engineer in the semiconductor industry (Transitron, 1960–1961, Clevite, 1961) and in the microwave industry (Raytheon, 1961–1966), specializing in high-power ferrite devices. He participated in the foundation of the Microwave Laboratory of the Catholic University of Louvain (1966–1970). Since 1970, he has been a professor at the Ecole Polytechnique Fédérale de Lausanne, directing the Laboratory of Electromagnetism and Acoustics (LEMA). He authored three textbooks on Electromagnetism and Microwaves (two in French, one in English) and some 150 publications dealing mostly with loaded waveguides, ferrite devices, and industrial applications of microwaves. He organized in 1974 the fourth European Microwave Conference in Montreux, Switzerland. He was Chairman of the IEEE Switzerland Section in 1975–1976, and served as reviewer for the IEEE TRANSACTIONS ON MICROWAVE THEORY AND TECHNIQUES for eight years. Since 1979, he has been Chairman of the Swiss National Committee of URSI and Swiss delegate to Commission B (Fields and Waves). He taught Microwaves at the Telecommunications Institute in Oran (Algeria) in 1979 and 1980 (ITU Missions), and was Visiting Professor at Ecole Polytechnique de Montreal, Canada, in 1978, and at the University of Delhi, India, in 1984. He is presently Chairman of the joint Swiss chapter of MTT-AP.